Energy, Mines and Resources Canada
Energie, Mines et Ressources Canada

CANMET
Canada Centre for Mineral and Energy Technology
Centre canadien de la technologie des minéraux et de l'énergie

THE EFFECT OF MECHANICAL DAMAGE ON FRACTURE INITIATION IN LINEPIPE PART II - GOUGES

K.C. Wang and E.D. Smith
Engineering Physics Section

MARCH, 1988

This document is an unedited interim report prepared primarily for discussion and internal reporting purposes. It may not represent a final expression of the opinion of the Canada Centre for Mineral and Energy Technology (CANMET)

Ce document est un rapport provisoire non révisé et rédigé principalement pour fin de discussion et de documentation interne. Il ne représente nullement l'expression définitive de l'opinion du Centre canadien de la technologie des minéraux et de l'énergie (CANMET)

METALS TECHNOLOGY LABORATORIES

24 pp

REPORT MTL 88-16(TR)

MICROMEDIA

88-02663/

METALS TECHNOLOGY LABORATORIES
REPORT MTL 88-16(TR)

THE EFFECT OF MECHANICAL DAMAGE ON FRACTURE INITIATION ON LINEPIPE
PART II - Gouges

by

K.C. Wang and E.D. Smith

ABSTRACT

The effect of mechanical gouges on the fracture of pipelines was evaluated by tensile tests of flattened transverse specimens with artificial defects as well as by pressurization tests of gouged pipe specimens.

The results of tests showed that tensile specimens with machined notches have a 15% higher notch strength (maximum nominal stress) than specimens without notches. Specimens with pressed notches have a 50% higher notch strength and specimens with gouges have notch strengths in between the two. Specimens with a gouge depth less than 22% will not fail in the gouged region.

The failure stress of linepipe with a gouge can be conservatively predicted by the Battelle flow stress dependent model of part-through flaws provided the maximum gouge depth and the corrected gouge length are used.

LABORATOIRES TECHNOLOGIQUE DES METAUX
RAPPORT MTL 88-16 (TR)

EFFET DE L'ENDOMMAGEMENT MÉCANIQUE SUR L'INITIATION DES FISSURES DANS LES TUBES DE CANALISATION
PARTIE II - Les rainures

par

K.C. Wang et E.D. Smith

RÉSUMÉ

Nous avons évalué l'effet des rainures mécaniques sur la rupture des pipelines en soumettant des échantillons transversals aplatis, comportant des défauts artificiels, à des essais de résistance à la traction, et des échantillons de tuyaux entaillés, à des essais de pressurisation.

Les résultats des essais démontrent que la résistance à l'effet d'entaille des échantillons pourvus de rainures mécaniques qui ont été soumis aux essais de traction, est de 15 % plus élevée (résistance nominale maximale) que celle des échantillons sans rainure. La résistance à l'effet d'entaille des échantillons qui ont des rainures pressées est de 50 % plus élevée tandis celle des échantillons comportant des rainures se situe entre les deux. La rupture ne se produira pas dans la zone rainurée des échantillons qui ont une rainure d'une profondeur de moins de 22 % de l'épaisseur de la paroi.

On peut prédire, d'une façon conservatrice, la contrainte de rupture dans les tubes de canalisation comportant des rainures. À cette fin, on peut utiliser le modèle Battelle qui est basé sur la contrainte d'écoulement des défauts à condition d'utiliser la profondeur maximale de la rainure et sa longueur corrigée.

INTRODUCTION

A study of gas pipeline failures between 1971 and 1975 showed that 56% of the failures were caused by mechanical damage (1). Damage was of three kinds: dents, gouges and gouges in dents. Studies at Battelle Columbus Laboratories (BCL) showed pipes with a dent will generally not break at the dent during burst testing (2). However, the failure stress is reduced when a notch is machined into a pipe surface and drastically reduced if a notch is machined at a dent on the pipe surface. Wade and Walsh tested sections of superficially damaged gas linepipe and found that the failure stress was still significantly higher than the design operating stress (3).

Standards on linepipe and on gas and oil pipelines pose stringent limitations to the damage (4,5,6). It has been the intent of this work to examine these requirements to ensure public safety and pipeline reliability without undue economic penalty from excessively conservative design.

In a previous report (7), the effect of dents alone was studied. The effect of gouges on linepipe will be reported here.

EXPERIMENTAL PROCEDURE

To understand how a gouge behaves on a pipe surface, transverse, artificially gouged tensile specimens were tested first. Transverse pipe segments 254 x 152 mm were machined and flattened from 508 mm diam, 5.65 mm wall thickness linepipes. Each piece was rigidly supported on a platen and gouged by a tool bit mounted on the tip of a pendulum. Four 25.4 x 254 mm tensile specimens with a transverse center notch were machined from each piece.

Tensile specimens from the same material were also prepared with machined or pressed U-notches. Wide specimens (101.6 mm compared with 25.4 mm) with a machined notch were prepared to provide more constraint across the specimen width. The geometries of these specimens are shown in Fig. 1.

Tensile specimens with or without gouges were tested in an MTS system with a loading rate around 10^{-3}/min. The tested specimens are shown in Fig. 2.

Pipe specimens for pressure testing, 2890 mm in length, were prepared from linepipe of nominal dimensions: diameter 508 mm (20"), thickness 5.56 mm (0.219", series FT) or 952 mm (0.375", series F). The chemical compositions and mechanical properties are shwon in Table 1. Before testing, each pipe was aligned beneath a pendulum to produce a gouge in the longitudinal direction. The F-series of pipes were gouged without internal support beneath the gouge; the FT series with a thinner wall required support.

Three gouges were formed on each pipe section, equally spaced, and offset 150 mm circumferentially from each other. End caps were welded on the pipe sections after gouging. The ligament thickness beneath the gouge was measured ultrasonically. To facilitate this, the gouging tool tips were modified so that the center of the gouge was flat so as to seat the ultrasonic probe properly. Because of slight deformation in the gouged region, ligaments measured by depth gauge were 0.5-0.7 mm smaller than when determined by ultrasonics. The gouge depth measured along the pipe axis was in reasonable agreement with the arc of the pendulum.

Pipe specimens were strain gauged in the gouge and on the pipe surface away from the gouge in both longitudinal and hoop directions. A clip gauge was also mounted across the gouge. Pipe specimens were tested with an MTS hydraulic test system capable of pressurizing the water-glycol mixture in the secondary circuit to 55 MPa. Each pipe specimen was pressurized monotonically to 110% of its yield pressure (i.e., 110% of the pressure to produce 0.5% hoop strain on the pipe wall) in 30 min.

Generally, cracks initiated at the corners (seen in transverse section) of each gouge and grew through the thickness as the pressure increased. A test was stopped if the deformation in the gouge or across the gouge increased rapidly, i.e., the pipe verged on failure. The gouge and the cracks were ground off and repair-welded. With 20FT-5, a thin-wall pipe, a burst segment was flame cut and patch repaired so that the remaining gouge could be further tested to failure.

One pipe specimen, 20FT-4, was pressurized to 110% of yield pressure (YP), then fatigue tested between 6% and 80% of the yield pressure for 7000 cycles when the pressure range was further increased from 6% to 90% of its yield pressure for another 2100 cycles.

RESULTS

TENSILE TEST

The results of tensile tests on strips with gouged, machined and pressed notches have been reported elsewhere (8) and are shown in Figs. 3, 4 and 5. Briefly, because of constraint in the groove direction the machine-grooved specimens have a notch tensile strength (maximum stress in the ligament) 15-17% higher than the tensile strength, $\sigma^{GM}(UT)$, of ungrooved specimens. The press-grooved specimens have a 50% higher notch tensile strength because of work hardening. The notch tensile strength of a gouged-groove lies somewhere between these two kinds of specimens. However, for a gouge depth less than about 22% of wall thickness, tensile specimens do not fail at the gouge but fail outside the gouge region as shown in Fig. 2.

PRESSURIZATION TEST

The results of pressurization tests are shown in Table 2. Three gouges were made in each pipe with the gouging tools noted in the table.

In the pressure testing of pipe specimen 20FT-4, no crack was detected after monotonic testing to 110% of yield pressure (YP), or the subsequent fatigue testing. This is understandable as the average gouge depth is only about 10% of the wall thickness and the gouge is of rounded shape. As reported above, a tensile strip with such a gouge of depth less than about 22% will not fail in the gouged section. It should be noted, however, that the stress system in a pipe is different from that in a tensile strip, and so the conditions controlling failure location will not necessarily be the same in the two cases. However, these observations show that a gouge of average depth of about 10% wall thickness can survive a test to 110% (of yield) hydrostatic pressure and subsequent operating pressure fluctuation for 9100 cycles.

The influence of tool shape was studied in pipe 20F-3. With a rounded tip (gouge #1), the pipe was deformed with little material being removed; a cross-section of the gouge is shown in Fig. 6. With a wide, flat-tipped tool (gouge #2), there was again little material removal. However, a white martensitic layer formed during scraping, as shown in Fig. 7. Although this layer cracked extensively during pressurization the cracks normally arrested in the deformed base metal. With a contoured tool

bit (rounded edges, flat bottom) (gouge #3), cracks formed at gouge corners as shown in Fig. 8. Two cracks are visible in Fig. 8, the larger one of which grew through the wall to burst the pipe.

Pipe specimen 20F-4 was pressurized until gouge #3 was on the verge of failing as indicated by a rapid increase in clip gauge displacement. This gouge was ground out and weld repaired. The process was then repeated for gouge #2. Finally, the pipe was pressurized until it burst at gouge #1, as shown in Fig. 9.

Pipe specimen 20FT-5 was tested to 7.58 MPa when it burst at #1 gouge. The fracture area was cut out and patch-welded with a 9.53 mm thick 508 mm diam pipe patch. The #3 gouge was tested to near break point then weld repaired. The #2 gouge was further tested to burst as shown in Fig. 10.

DISCUSSION

Kiefner et al. at Battelle Columbus Laboratories (BCL) studied flaws machined into pipe walls (9). From this work, equations were derived to predict the stresses at which surface flaws induced failure in pressurized cylinders using two models.

1. For the "flow stress dependent" model

$$\sigma = \bar{\sigma} \left(\frac{1 - d/t}{1 - d/M_t t} \right)$$

where: σ = hoop stress level at failure

$\bar{\sigma}$ = flow stress = yield stress + 69 MPa

d = depth of notch

t = pipe wall thickness

M_t = Folias correction factor

$$= \left(1 + 1.255 \frac{c^2}{Rt} - 0.0135 \frac{c^4}{R^2 t^2} \right)^{1/2}$$

2. For the "toughness dependent" model

$$\left(\frac{12\, C_v}{A_c} \right) \left(\frac{E\, \pi}{8 C_{eq} \bar{\sigma}^2} \right) = \ln \sec \frac{\pi}{2} \left(\frac{M_t \sigma}{\bar{\sigma}} \right)$$

or

$$\sigma = \frac{\bar{\sigma}}{M_p} \frac{2}{\pi} \sec^{-1} \exp\left(\frac{3\, C_v\, E\, \pi}{A_c \cdot 2C_{eq} \cdot \bar{\sigma}^2}\right)$$

where: $M_p = (1 - d/t) \,/\, (1 - d/M_t \cdot t)$

C_v = 2/3 Charpy V-notch toughness

$2C_{eq} = A/d$

A = actual area of the surface flaw.

A_c = area of 2/3 Charpy specimen below notch

In a longitudinal notch machined with a milling cutter, the depth of the notch is uniform along its length except at both ends where the notch has the same radius as that of the cutter tool. In a gouge, the depth is not uniform. Calculations with (a) original gouge length 2C and maximum gouge depth d_{max}, (b) corrected gouge length $2C_{eq}$ and d_{max} and (c) 2C and average gouge depth d_{ave} were carried out to determine the failure stresses shown in Table 3. In addition to these three sets of assumptions concerning gouge geometry, two values for $\bar{\sigma}$, the flow stress, were used in calculating σ, the failure stress. Although the yield stress for pipe specimens 20F3 and 20F4 determined by the pipe mill was 418 MPa, a yield stress of 464 MPa was measured by tensile testing of 25.4 mm wide flattened specimens; these two values of yield stress lead to flow stress values of 487 and 533 MPa. Each value of failure stress σ, calculated by these different sets of assumptions has its own nomenclature which is described in the footnotes to Table 3 and on p.9.

As the results given in Table 3 indicate, failure stresses calculated by the fracture toughness dependent model are low (conservative). Calculated stresses based on the flow stress model give results closer to those observed.

The differences in behaviour induced by gouges and notches are listed in Table 4. Cracks were observed to initiate in the martensitic layer of a gouge but arrested at the deformed layer. At high stresses, cracks at the corner of a gouge propagated through the deformed layer into the parent metal. It may be inferred that the dynamic initiation effect is

insignificant when a test is performed at temperatures where the pipe material is in the upper shelf region as is likely in the present case. A further comparison of the actual failure stress for pipes with gouges with the Battelle predicted value based on a machined sharp notch is shown in Table 5 and Fig. 11. The estimates are conservative in almost all cases, ranging between 69% and 106% of measured burst pressure.

CONCLUSIONS

1. When a linepipe has a 2/3 CVN energy above 20 J, the martensitic layer and the deformed layer associated with a gouge do not degrade a pipe more than a pipe with the same size of machined notch.
2. For gouges up to 15% wall thickness which do not possess a hardened martensitic layer but only a deformed layer, a crack will not form even if it is stressed beyond its yield point. The Battelle models underestimate failure stress.
3. The Battelle flow stress dependent model for surface flaws on linepipe can be used to predict the failure stress of pipes with a gouge, provided the maximum crack length and average crack depth are used. With these assumptions, the model gives a slightly conservative estimate.

REFERENCES

1. Smith, R.B. and Gideon, D.N. "Statistical analysis of DOT-OPSO data"; AGA 6th Symposium on Linepipe Research; Houston, Texas; 1979.

2. Symposium on Linepipe Research; AGA Catalogue No. L30 000; November 1965.

3. Wade, J.B. and Walsh, D.T. "Hydrostatic testing of damaged gasoline pipe"; Australia Welding Research; December 1977.

4. CSA Standard Z-245.1-M1982; General Requirement for Plain-end Welded and Seamless Steel Linepipe.

5. CSA Standard Z183-M1982; Oil Pipeline Transportation Systems.

6. CSA Standard Z184-M1983. Gas Pipeline Systems.

7. Wang, K.C., and Smith, E.D. "The effect of mechanical damage on fracture initiation in line pipe"; Part I - Dents. Report ERP/PMRL 82-11(TR).

8. Wang, K.C., Roy, G. and Tyson, W.R. "Plastic collapse stresses of plates with surface grooves"; CFC10; Modelling Problems in Crack Tip Mechanics; Waterloo, Ontario. Martinus Nijhoff Publishers, pp.335-344. Report ERP/PMRL 83-32 (OP-J), August 1983.

9. Kiefner, J.F., Maxey, W.A., Eiber, R.J. and Duffy, A.R. "Failure stress levels of flaws in pressurized cylinders"; ASTM STP536; Progress in Flaw Growth and Fracture Toughness Testing; 461-481; 1973.

NOMENCLATURE

A = actual area of a surface flaw

$2C$ = measured crack length

$2C_{eq}$ = equivalent crack length = A/d_{max}

C_v = 2/3 Charpy V-notch energy

d = depth of gouge or other type of defects

d_{ave} = average gouge depth = $A/2C$

d_{max} = maximum gouge depth

D = pipe diameter

ϵ_{hp} = hoop strain in the pipe surface

20F = pipe specimen with 508 mm diam, 9.53 mm nominal wall thickness

20FT = pipe specimen with 508 mm diam, 5.56 mm nominal wall thickness

M_t = Folias correction factor = $\left(1 + 1.255 \frac{C_{eq}^2}{Rt} - 0.0135 \frac{C_{eq}^4}{R^2 t^2}\right)^{1/2}$

P = pressure

R = pipe radius

σ_d = design stress = 80% specified minimum yield stress

σ_{hp} = hoop stress = $PD/2t$

σ_{F1} = flow stress dependent failure stress

σ_{F2} = toughness dependent failure stress

σ_M = maximum tested stress at or before failure

σ_{Mop} = stress at maximum operating pressure

σ_u = estimated failure stress of pipes without any defects

t = pipe wall thickness

Table 1 - Chemical composition and mechanical properties of pipes tested

Pipe designation	Composition, wt %								YS	UTS	El	2/3 CVN
	C	Mn	P	S	Si	Cb	Cr	Ce	MPa	MPa	%	J
20F	.19	1.09	.007	.013	.20	.01	-	-	418 464+	567	34	25
20FT	.18	.72	.006	.028	.06	-	.06	.30	415	520	28	21*

+Measured using a flattened strip specimen

*Calculated from the results of half-size specimens assuming absorbed energy proportional to ligament area.

Table 2 - Pressurization tests of pipe specimens with gouges

Specimen No.	Gouge No.	Gouging tool	Gouge depth d_{max} mm	Gouge depth d_{ave} mm	Gouge length mm	t mm	P MPa	σ_{hp} MPa	ϵ_{hp} %	$\frac{d_{max}}{t}$ %	$\frac{d_{ave}}{t}$ %	Results
20FT-4	1	R	.99	.62	254	5.56	9.51	434*	.94	17.8	11.1	no crack
	2	R	1.19	.49	254	5.56	.4-7.17	434*	.94	21.4	8.8	no crack
	3	R	1.04	.61	254	5.56	.4-7.86	434*	.94	18.7	11.0	no crack
20F-3	1	R	1.55	1.24	247	9.65	19.75	520	.2	16.1	12.8	no crack
	2	F	1.32	.97	156	9.65	19.75	520	.2	13.7	10.1	surface crack formed
	3	C	2.39	1.85	162	9.65	19.75	520	.2	24.8	19.2	burst
20F-4	1	C	1.8	1.0	190	9.88	20.2	532	0.635	18.7	10.4	burst
	2	C	2.01	1.04	200	9.88	19.2	505	0.185	20.8	10.8	near failure, gouge repaired
	3	C	2.13	1.1	200	9.88	18	474	0.17	22.1	11.4	near failure
20FT-5	1	C	2.54	1.85	179	5.56	7.58	386	.144	45.7	33.3	burst, patched
	2	C	1.98	1.19	180	5.56	8.89	406	.26	35.6	21.4	near failure, gouge repaired
	3	C	2.21	1.35	185	5.56	8.55	390	.178	39.7	24.3	burst

*Monotonically loaded to 434 MPa then fatigued between 18.3-326 MPa for 7000 cycles, between 18.3-359 MPa for 2100 cycles.

Tool shapes: R (rounded tip, ~6 mm radius of curvature, and 6 mm width)

F (flat edged 12.7 mm width)

C (contoured, ~6 mm radius of curvature with 3.2 mm flat ground on bottom edge, (6 mm width)

Table 3 - Failure stress levels of pipes and gouges

Pipe	Gouge No.	†	d_{max} mm	2C mm	$2C_{eq}$ mm	d_{ave} mm	σ_M MPa	σ_{F1} MPa	σ_{F2} MPa	σ_{F1}' MPa	σ_{F2}' MPa	σ_u MPa	Results
20F-3	1	(a)	1.55	247			>527	474	378	433	364	588	no crack
		(b)	1.55		197			470		440			
		(c)		247		1.24		486	380	444	374		
20F-3	3	(a)	2.30	162			527	455	406	416	384	588	burst
		(b)	2.30		126			468		428			
		(c)		162		1.85		474	423	434	400		
20F-4	1	(a)	1.8	190			519	471	380	430	398	588	burst
		(b)	1.8		106			494		451			
		(c)		190		1.0		499	403	456	422		
20F-4	2	(a)	2.01	200			493	463	374	423	391	588	near failure
		(b)	2.01		103			490		450			
		(c)		200		1.04		498	403	455	421		
20F-4	3	(a)	2.13	200			474	462	372	422	390	588	near failure
		(b)	2.13		103			487		445			
		(c)		200		1.1		496	401	453	440		
20FT-5	1	(a)	2.54	170			346	315	280			539	burst
		(b)	2.54		130			334					
		(c)		170		1.85		367	337				
20FT-5	2	(a)	1.98	180			406	358	328			539	burst
		(b)	1.98		108			385					
		(c)		180		1.10		412	378				
20FT-5	3	(a)	2.21	185			390	339	309			539	near failure
		(b)	2.21		113			367					
		(c)		185		1.35		401	366				

σ_M = maximum tested stress

σ_{F1} = flow stress dependent failure stress ($\bar{\sigma}$ = 533 MPa from mill test)

σ_{F1}' = flow stress dependent failure stress ($\bar{\sigma}$ = 487 MPa from measured yield stress)

σ_{F2} = toughness dependent failure stress ($\bar{\sigma}$ = 533 MPa)

σ_{F2}' = toughness dependent failure stress ($\bar{\sigma}$ = 487 MPa)

σ_u = estimated failure stress of pipe without defects

† = values used in the calculation:

(a) d_{max}, 2C; (b) d_{max}, $2C_{eq}$; (c) d_{ave}, 2C

Table 4 - Comparison of characteristics of a machined flaw (notch) with a gouge

Machined notch	Gouge
1. Relatively sharp notch root	1. Similar to contour of tool bit.
2. No work hardening at root	2. Martensitic, heavily deformed layer at root.
3. Uniform notch depth	3. Depth not uniform.
4. Crack initiates and grows from the root of mechanical notch	4. Cracks initiate in martensitic layer, then arrest. At higher stress, cracks extend through deformed layer. Dynamic crack initiation in martensitic layer insignificant at upper shelf.

Table 5 - Comparison of actual versus predicted failure stress

Gouge No.	†	σ_M MPa	σ_{F1}/σ_M %	σ_{F1}'/σ_M %	σ_{F2}/σ_M %	σ_{F2}'/σ_M %
20F-33	(a)	527	86.3	78.9	71.7	69.1
	(b)		88.8	81.2		
	(c)		89.9	82.4	73.8	71.0
20F-41	(a)	519	90.8	82.9	76.7	73.2
	(b)		95.2	86.9		
	(c)		96.1	87.9	81.3	77.6
20F-42	(a)	493*	93.9	85.8	79.3	75.9
	(b)		99.4	91.3		
	(c)		101.0	92.3	85.4	81.7
20F-43	(a)	474*	97.5	89.0	82.3	78.5
	(b)		102.7	93.9		
	(c)		104.6	95.6	92.8	85.0
20FT-51	(a)	346	91.0		83.5	
	(b)		96.5			
	(c)		106.1		97.4	
20FT-52	(a)	406	88.2		80.8	
	(b)		94.8			
	(c)		101.5		93.1	
20FT-53	(a)	390*	86.9		79.2	
	(b)		94.1			
	(c)		102.8		93.8	

*Pipe specimens pressurized close to failure. The actual failure pressure and stress will be higher hence the ratio will be lower

†Values used in the calculation

(a) d_{max}, 2C

(b) d_{max}, $2C_{eq}$

(c) d_{ave}, 2C

σ_M, σ_{F1}, σ_{F2}, σ_{F1}', and σ_{F2}' - same as in footnote, Table 3.

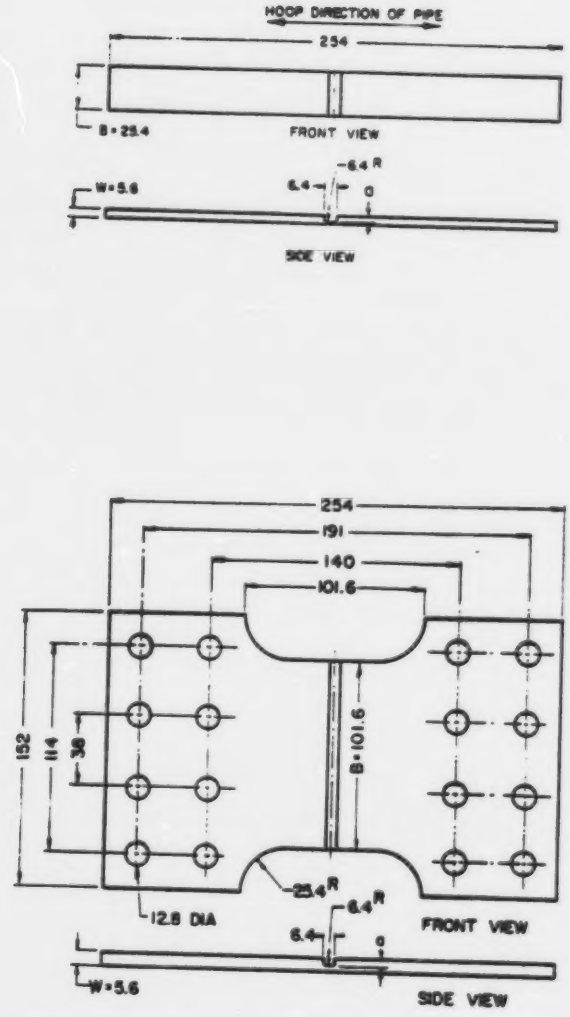

Fig. 1 Dimensions of tensile specimens with machined notches. (neg 8612, 8614)

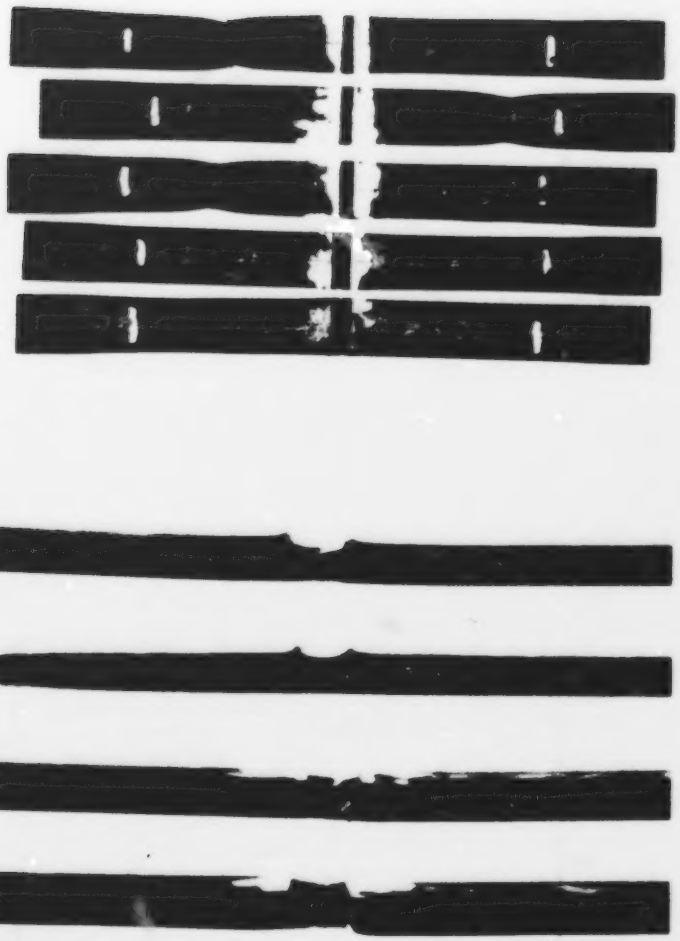

Fig. 2 Tensile tested transverse flattened pipe specimens with center gouge. Note that the upper three specimens failed outside the gouged region; for these specimens, $d/t \lesssim 0.2$. (neg. 4866, 4884)

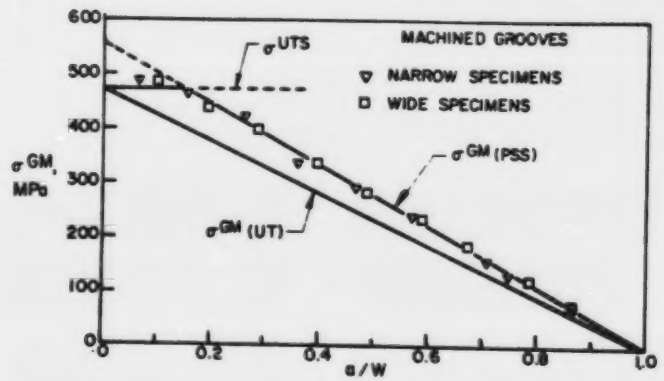

Fig. 3 Failure stress of tensile specimens with machined grooves σ^{GM} (PSS) and without grooves σ^{GM} (UT). (neg. 8613)

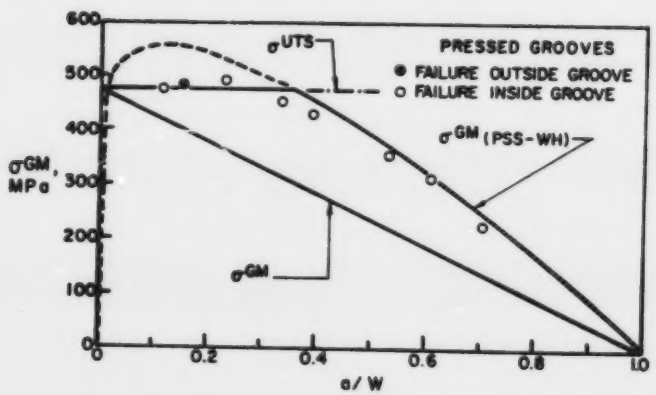

Fig. 4 Failure stress of tensile specimens with pressed notches σ^{GM} (PSS-WH). (neg. 8610)

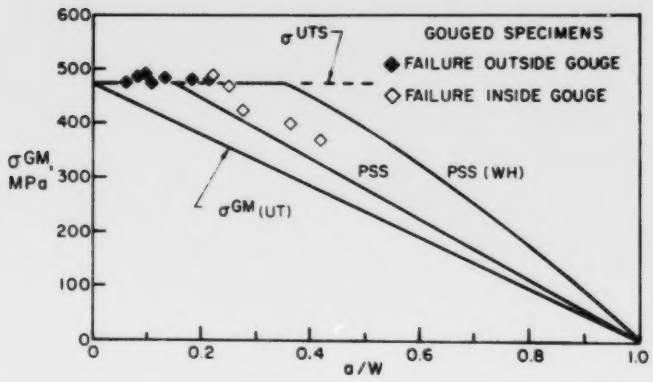

Fig. 5 Failure stress of tensile specimens with gouges. (neg. 8607)

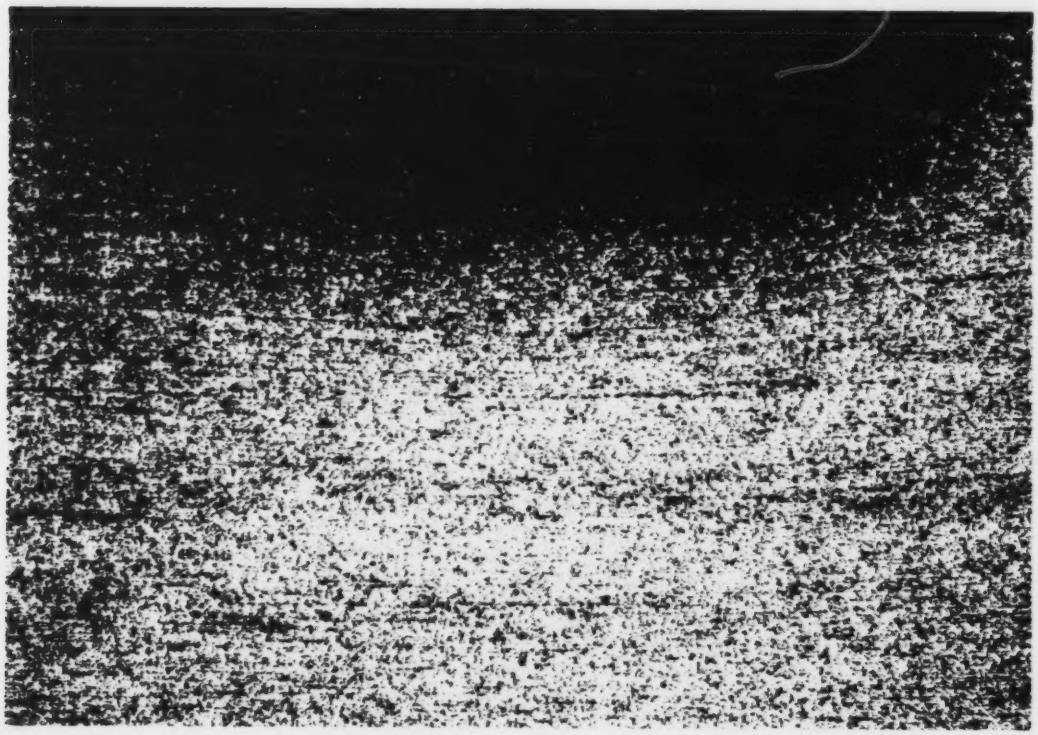

Fig. 6 Pipe specimen 20F-3, gouge #1 12.7 x. (neg. 17094)

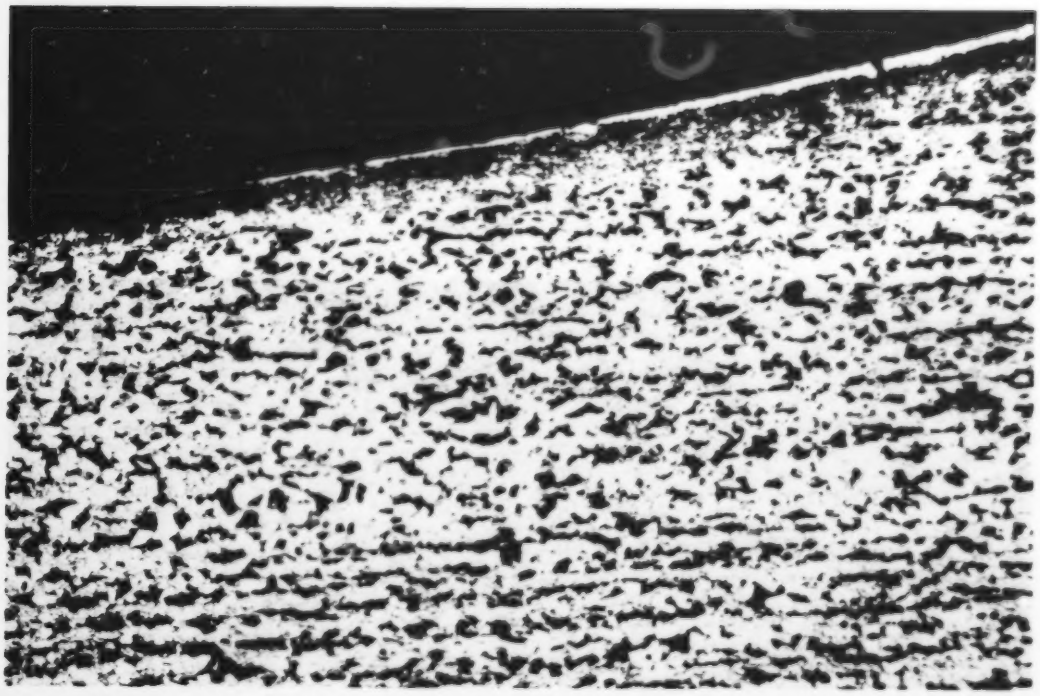

Fig. 7 20F-3, gouge #2. Crack initiated in the white martensitic layer but did not grow into the deformed layer nor base material. 200 x. (neg. 17095)

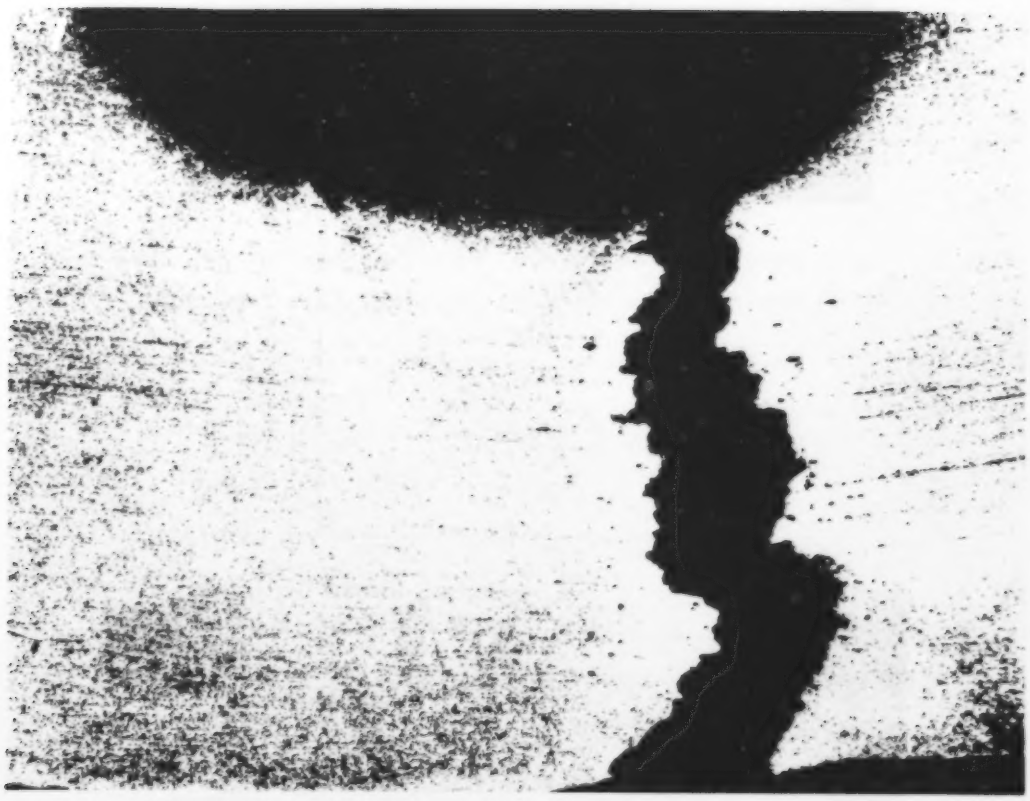

Fig. 8 Pipe specimen 20F-3 gouge #3. Cracks initiated at the corners of the gouge. One grew through the thickness to burst the pipe. 12.7 x. (neg. 17096)

Fig. 9 Burst pipe specimen 20F-4. The other two notches have been weld-repaired (indicated by the arrows). (neg. 8883)

Fig. 10 Tested pipe specimen 20 FT-5. Left gouge was repair welded, center gouge was burst then patch-welded with a thicker wall pipe, and right gouge was also burst. (neg. 9043)

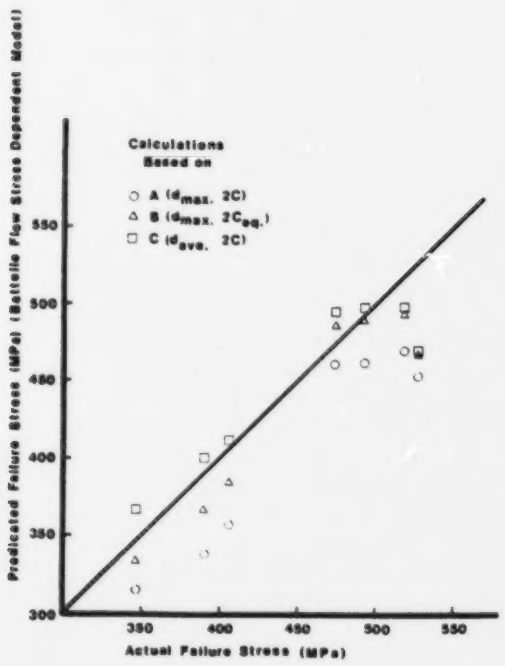

Fig. 11 Actual failure stress vs predicted failure stress using the Battelle flow stress dependent model for surface flaws. (neg. 14952)